

Central European Journal of Chemistry

Study by grazing incident diffraction and surface spectroscopy of amalgams from ancient mirrors

Research Article

L.K. Herrera^{1*}, A. Duran², M.L. Franquelo¹, A.R. González-Elipe¹, J.P. Espinós¹, J. Rubio-Zuazo³, G. R, Castro³, A. Justo¹, J.L. Perez-Rodriguez¹

¹ Materials Science Institute of Seville (CSIC-US), 41092 Seville, Spain.

² Centre for Research and Restoration of the Museums of France – CNRS, Paris. France

³ Spanish CRG beamline SpLine at the ESRF, F-38043 Grenoble, France

Received 04 July 2008; Accepted 15 October 2008

Abstract: Characterization of four amalgam surfaces, with different alteration degrees from Andalusia historical mirrors, has been carried out by grazing-incidence X-ray diffraction (GIXRD), and other spectroscopic techniques (SEM/EDX, XPS, and REELS). The combination of all these techniques allows determining the corrosion state of the amalgams. The results show that the amalgams are composed in all cases of a binary alloy of tin and mercury. As mercury has high vapour pressure at RT, it slowly segregates and eventually evaporates, it leaves finely divided particles of tin that easily can be oxidize, forming tin monoxide (SnO) and tin dioxide (SnO₂). In one of the samples, most of the amalgam remains unoxidized, since Hg_{0.1}Sn_{0.9} and metallic Sn phases are the major components; in two other samples, Hg_{0.1}Sn_{0.9} and Sn phases are not detected while SnO₂ and SnO phases appear. Finally, in the last studied sample, only SnO₂ phase is detected. The surface analyses of these samples by XPS show that, for most of them an unique chemical species (Sn⁴⁺) is found.

Keywords: Tin oxides • corrosion process • XPS • REELS GIXRD • Ancient mirrors

© Versita Warsaw and Springer-Verlag Berlin Heidelberg.

1. Introduction

A pane of glass backed with a tin-mercury amalgam, commonly called the amalgam mirror, was the most used mirror from the sixteenth century until the beginning of the twentieth [1, 2]. It is difficult to determine when the tin amalgam mirror processing technique was discovered; however, the first known production centre for these mirrors was opened in Venice in 1507 by the Dal Gallo brothers from Murano Island [2]. They had developed a new method to make mirrors [3, 4] using a tin-mercury amalgam comprised of a two-phase system in which crystals of tin-mercury compounds were surrounded by a mercury rich liquid phase.

The Venetian mirror industry dominated the market until the middle of seventeenth century. The glass for Venetian mirrors was blown using cylinder methods

and it proved difficult to fashion objects longer than one meter [3]. The reflecting layer of mercury on these mirrors was composed of approximately 75% tin and 25% mercury. The name "tin mirror" would therefore be more appropriate. The production of amalgam mirrors was difficult because the application of amalgam backing needed a lot of mercury and its vapour made the work very unhealthy. In the middle of the nineteenth century, production of silver-backed mirrors began; the new method was quicker and safer, but the silver mirrors were not as durable. In the first decades of the twentieth century, amalgam mirrors were still being produced [4].

Corrosion of the tin-mercury alloy surface of amalgam mirrors produces tin dioxide and tin monoxide and releases mercury from the amalgam solid phase. The Sn^o can be altered to SnO and SnO₂ [5]. These two tin oxides

^{*} E-mail: Ikaren@icmse.csic.es

are the normal products of atmospheric corrosion of tin-containing objects, i.e. tin, tin alloys, bronze, amalgams, and pewter artefacts [6,7,8,9]. SnO generally has an anthropogenic origin, commonly being derived from the corrosion of tin artefacts in a marine environment [10]. SnO₂ is by far the most typical and most stable corrosion product of tin. The SnO₂ layer is formed passivating the surfaces in the environments studies [11]. In the corrosion-inhibitive effect, amorphous tin oxide is assumed to form a protective barrier on bronze surfaces [12]. In this paper we show that mercury releases produce very small particles of tin that are then oxidized. The oxidation grade is strongly dependent on the surrounding environment. In order to gain further insight into these surfaces, the most appropriated techniques are Grazing-Incidence X-ray Diffraction (GIXRD), Scanning Electron Microscopy, combined with an X-ray energy dispersive spectrometer (SEM/EDX), and Surface-Spectroscopic Methods including X-ray Photoelectron Spectroscopy (XPS) and Reflection Electron Energy Loss Spectroscopy (REELS). GIXRD is a valuable technique that provides very precise information on surface and interface atomic arrangements in crystalline structures [13,14,15,16]. By varying the angle of incidence, the penetration of the X-ray beam into the material can be controlled, allowing the acquisition of non-destructive crystalline composition depth profiles, as well as the analysis of surfaces and buried interfaces.

X-ray photoelectron spectroscopy (XPS) and reflection electron energy-loss spectroscopy (REELS) are powerful surface-sensitive analytical techniques that are well suited for the analysis of materials. The corrosion products of the tin mercury alloy are SnO and SnO $_2$. Some difficulties have been showed for characterizing the chemical state of Sn oxides using XPS. However, Jimenez *et al.* [17] report the preparation of SnO $_2$ and SnO thin films and their characterization by surface-spectroscopic methods.

This research is focused on characterization of the amalgams present in the surfaces of four mirrors (XVIIth – XVIIIth century), with different alteration degrees, from Andalusia historical buildings. The combination of GIXRD, XPS and REELS techniques is able to clearly determine the corrosion state of the mirrors.

1.1 Materials

Four mirrors used for baroque ornamentation have been studied in this work (Fig.1). The samples were collected by taking a small pane of the amalgam from these mirrors (see Table 1). The mirrors were dated between the XVII and XVIII centuries.

Table.1. Description of the mirrors

Sample	Century	Location and description
1	XVII	The samples were obtained from the Hermitage of the "Cristo del Llano" (17th Century), which is located in a village of the northern district of Jaen, in the middle of the Sierra Morena mountains. The mirror was mounted in the wood frame of a large baroque altarpiece. The amalgam layer was scarcely corroded. The environment was classified as a rural atmosphere.
2	XVIII	The samples were taken from the "Santa Ana" parish church in Seville. The mirror was mounted in a wooden frame, and its back was covered with a wooden panel. The dust behind the mirror contained drops of mercury. The amalgam layer was corroded. The environment was classified as an urban atmosphere; however, in the past, it was an industrial atmosphere with ceramic factories.
3	XVIII	The samples were acquired from mirrors of the "Santiago" church in Écija. The mirror was mounted in a wooden frame. The amalgam layer was completely corroded and no longer adhering to the glass. The environment was classified as an urban atmosphere that was exposed to very high temperatures in the summer.
4	XVIII	The samples were acquired from "Camerin Virgen del Rosario" in the Santo Domingo Convent in Granada. The mirror fragments were enclosed in different frames of baroque ornamentation in the Camerin, and the back side of the mirror was in contact with a gypsum wall. The amalgam layer was completely corroded. The environment was classified as an urban atmosphere.

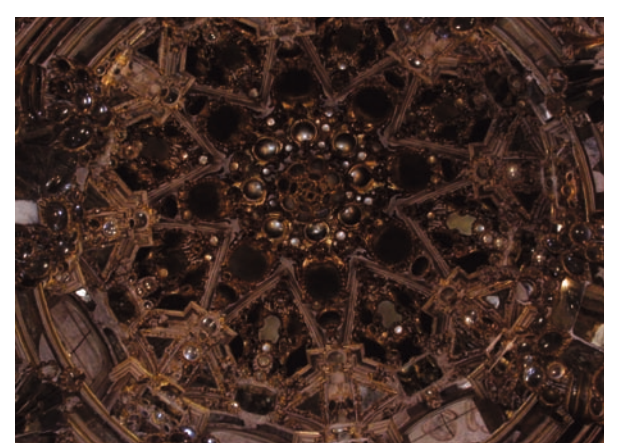


Figure 1. Photografy of Sample 4: Camerin Virgen del Rosario in the Santo Domingo Convent (Granada)

2. Experimental Procedures

The morphology was observed using an HITACHI S-4800 Scanning Electron Microscope. The elemental analysis of the amalgam was carried out in a JEOL JSM5400 electron microscope, using an X-ray energy dispersive spectrometer EDX Link ISIS.

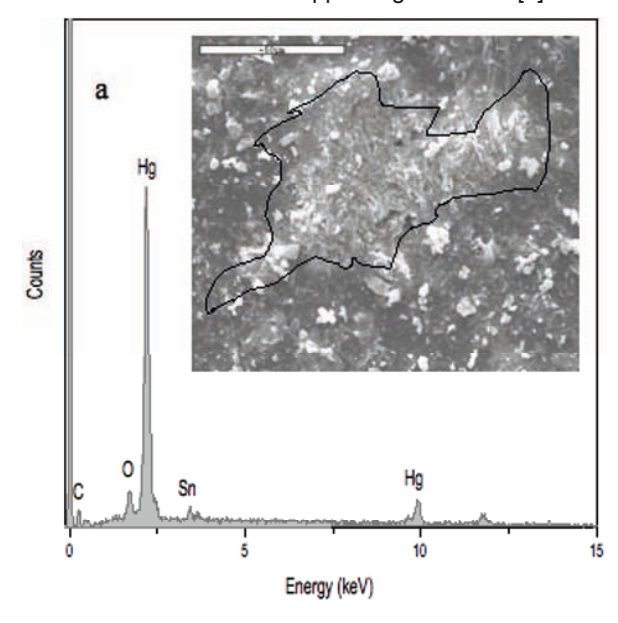
Grazing-incidence X-ray Diffraction was performed at the six-circle diffractometer installed at SpLine, the Spanish CRG beamline at the European Radiation Facility (ESRF) [16]. Diffraction measurements were performed using the constant grazing incidence geometry with a fixed energy of 14 KeV (wavelength 0.855 Å). The vertical geometry was used in order to take advantage of both the linear polarization of the bending magnet synchrotron radiation and the low beam vertical divergence. The set-up used (diffractometer + X-Ray beam divergence) provides an incident angle accuracy of 5 × 10⁻³ degrees, which enables an accurate control of the sampling depth. The incidence angle was varied between 0.4 and 3 degrees in order to change the penetration depth from a few nanometers up to several micrometers. The X-Ray beam spot size was 300 µm (horizontal) × 500 µm (vertical), allowing discrimination between the amalgam and corroded regions of the samples.

GIXRD has become well established for the investigation of the structure of films, surfaces and interfaces [18-21]. In the grazing incidence geometry, X-ray beams impinge on the surface at small incidence angles (ϕ). For all materials, the refractive index at X-ray energies is slightly less than one, and there is a critical angle ϕ_c below which total external reflection occurs. For incidence angles lower than ϕ_{s} , the X-rays are evanescent within the solid and penetrate only few Angstroms. As the incident angle increases and becomes equal to ϕ_c , the X-ray penetration depth (Λ) rapidly increases, and for an incidence angles above ϕ_{c} , it approaches several microns, as expected from the X-ray absorption coefficient. Consequently, the diffracted beams originate in regions of variable depth when the incidence angle is changed. Diffraction patterns as a function of incidence angle therefore allow construction of composition depth profiles of the crystalline phases.

The XPS and REELS spectra were recorded on an ESCALAB 210 spectrometer operating in the pass energy constant mode at 50 eV for XPS and at 20 eV for REELS. The base pressure during measurements was typically 5 \times 10 $^{-10}$ Torr. Al K α radiation was used as excitation source. The binding energy scale was referenced by using the Sn 3d $_{\rm 5/2}$ peak at 487.55 eV. The sensitivity factors from the apparatus were used for the quantification of the XPS spectra.

3. Results and discussion

The SEM/EDX analysis of Sample 1 shows two phases in the amalgam: a mercury-rich liquid phase (Fig. 2a) and a tin-mercury solid phase (Fig. 2b). The heterogeneous corroded surfaces of Samples 2 and 3 also show the presence of Hg and Sn (Fig. 3). Hg was mainly found on top of the crater-shaped holes (Fig. 3a-c) and Sn was the main component (Fig. 3d). The EDX analysis of Sample 4 shows the presence of Sn on the surface, while Hg was not found. Ca, Si, C and O were also detected, with their presence attributed to environmental contamination (Fig. not shown). Mercury is volatile and could be disappearing over time [2].



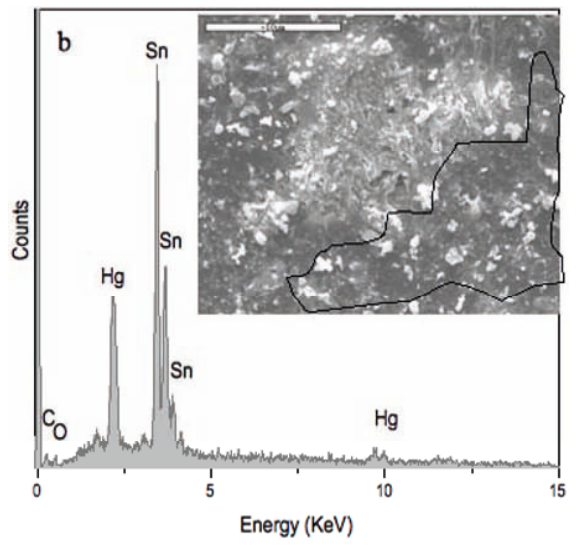


Figure 2. SEM/EDX analysis of the phases present in Sample 1: (a) mercury rich liquid phase; (b) tin-mercury solid phase.

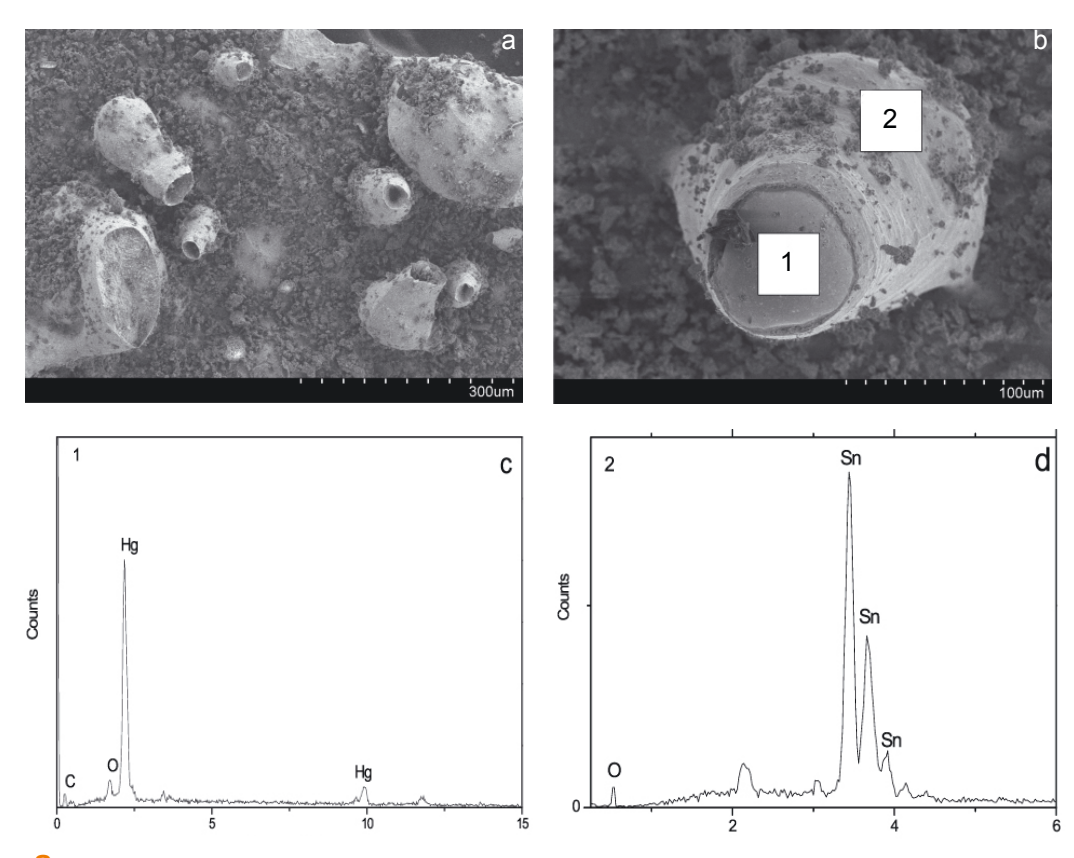


Figure 3. SEM microphotography of the heterogeneous corroded surfaces of the amalgam: (a) Sample 2, (b) Sample 3, (c) EDX analysis of a Hg drop on top of the craters-shaped holes, (d) EDX analysis of the craters-shaped.

In GIXRD measurements, the penetration depth (Λ) of the beam is dependent on the wavelength and incidence angle and is calculated from the Beer-Lambert law [22]. For calculating the penetration depth (Λ) of the beam into the sample, it is necessary to know the critical angles (\(\phi_c\)) for different compounds found on the surface of the amalgams. The calculated critical angles, for the four phases observed, namely β-Sn, $Hg_{0.1}Sn_{0.9}$, SnO, and SnO₂, are: $\phi_c \beta Sn = 0.20$ $\phi_c Hg_{0.1}Sn_{0.9} = 0.67$, $\phi_c SnO_2 = 0.20$ and $\phi_c SnO = 0.19$ (calculated following the work of Toney et al. [23]). Although the critical angles of three phases present in the samples are around 0.2°, a minimal incidence angle of 0.4° has been choosen due to sample roughness variations of the order or higher than 0.2° are expected. The GIXRD measurements were obtained at ϕ of 0.4°, 0.5°, 0.8°, 1° and 3° incidence angles, corresponding to a penetration depth ranging between 0.4 and 4 µm [24]. The penetration depth has been calculated as the layer thickness which contributes to 92% of the total diffracted signal. Fig. 4 shows the diffraction patterns of Sample 1 for increasing incidence angles. Two different phases can be distinguished. The GIXRD shows the presence of Hg_{0.1}Sn_{0.9} according

JCPDS files (481546, 40673 respectively) [2.99 Å (001), 2.78 Å (100), 2.0.4 Å (101) 1.60 Å (110) 1.39 Å (200)]. In addition, diffractions corresponding to β-Sn appear [2.91 Å (200), 2.79 Å (101), 2.06 Å (220), 2.02 Å (211), 1.66 Å (301), 1.48 Å (112), 1.44 Å (321)]. The GIXRD patterns show similar characteristic peaks and intensities at different incidence angles. These data suggest a similar composition along the depth profile, associated with a low degradation of the amalgam layer. Figs. 5 and 6 show the GIXRD patterns of the Samples 2 and 3. SnO₂ [3.35 Å (110), 2.64 Å (101), 2.37 Å (200), 1.76 Å (211). 1.67 Å (220), 1.50 Å (310)] and SnO [2.99 Å (101) 2.69 Å (110), 1.80 Å (112), 1.60 Å (211)] phases appear, while Hg_{0.1}Sn_{0.9} and β-Sn phases were not found, suggesting higher corrosion of these samples. Important changes in the phases along the depth profile at different incident angles were not detected. The diffraction peaks obtained with $\phi = 0.4^{\circ}$ are broader than those obtained with $\phi = 3^{\circ}$, which can probably be attributed to the less crystalline tin oxides phases approaching the sample surface. This fact is due to the higher alteration at the top of the amalgam layer. From the analysis of the relative intensity of different peaks (phases), it is possible to obtain information about the different alteration degree in both samples. The intensity ratios of the 3.39 $\rm \AA$ (SnO₂) and 2.29 $\rm \AA$ (SnO) peaks, as obtained from X- ray diagrams of both samples, show higher values for sample 3, in agreement with a higher SnO₂ concentration.

In the depth profile obtained by GIXRD measurements for sample 4, only the SnO_2 phase is observed (Fig. 7). The presence of only SnO_2 confirms that this sample shows the highest alteration degree of all the samples studied in this work. Most probably, the initially formed SnO phase changed with the time to yield the most

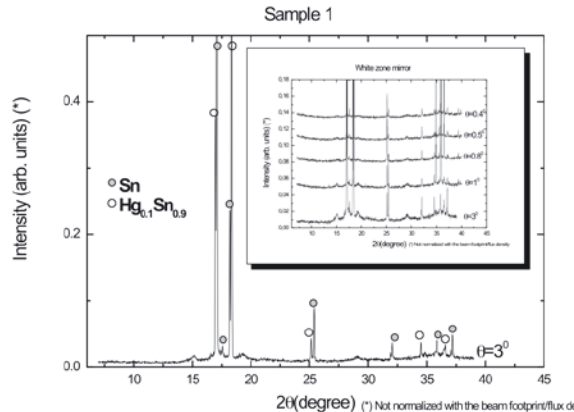


Figure 4. XRD profiles at different incidence angle $\phi=0.4^{\circ}$ to 3° of Sample 1

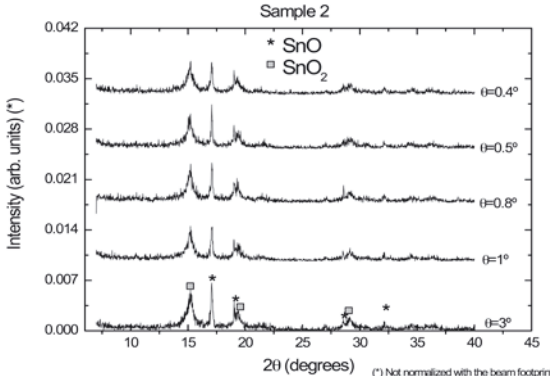


Figure 5. XRD profiles at different incidence angle $\phi = 0.4^{\circ}$ to 3° of Sample 2

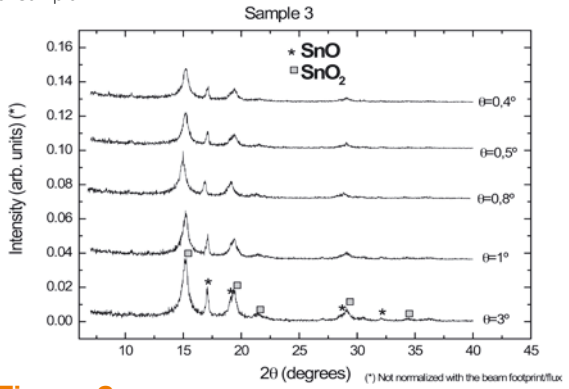


Figure 6. XRD profiles at different incidence angle $\phi = 0.4^{\circ}$ to 3° of Sample 3

thermodynamically stable SnO_2 phase. In addition $[CaSO_4 \cdot 2H_2O]$ 7.63 Å was also present in very low proportions, due to environmental indoor contamination. It is well known that sulphates contribute to increase the corrosion rate of the amalgams [25].

The X-ray photoelectron spectra of the amalgam surfaces are shown in Fig. 8. The core-level lines Sn4d, Sn4s, C1S, Sn3d, O1S, Sn3p_{3/2}, Sn3p_{1/2}, and the Auger lines SnMNN and OKVV can be seen clearly for Samples 1, 2 and 3. Similar core-levels appear in Sample 4, together with Si2p, Si2s, S2p and Ca2p.

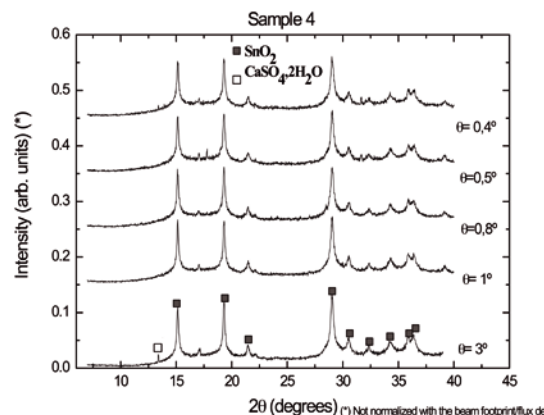


Figure 7. XRD profiles at different incidence angle $\phi=0.4^{\circ}$ to 3° of Sample 4

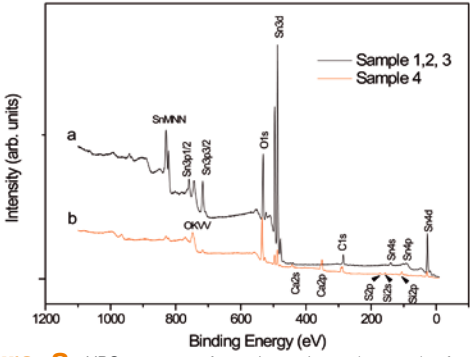


Figure 8. XPS spectra of amalgam layer (~5 nm) of samples: (a) Samples 1, 2, and 3, (b) Sample 4.

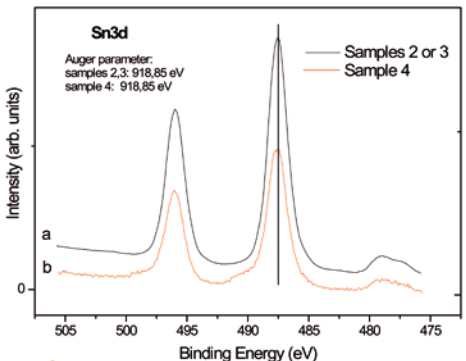


Figure 9. Sn 3d photoelectron peaks for: (a) Samples 2 or 3, (b) Sample 4

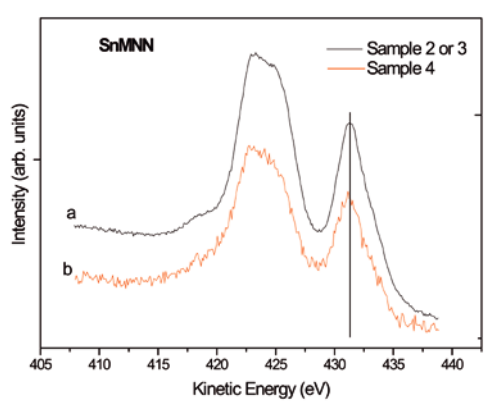


Figure 10. Sn Auger peaks of amalgam surface in Samples 2, 3 and 4

Hg traces have not been detected by XPS (Fig. 8). This fact suggests that Sn could be enriched in the outer layer of the amalgam, whereas Hg remains in deeper layers that are not reached by the XPS radiation.

The surface analysis of Samples 2 and 3 by XPS shows a unique chemical species for tin: Sn4+. This species is characterized by a Sn 3d_{5/2} peak at 487.55 eV of binding energy (Fig. 9) and a SnMNN Auger peak at 431.30 eV of kinetic energy (Fig. 10) (modified Auger parameter, 918.85 eV). These energetic values confirm that, at the surface, tin is oxidized to SnO or SnO₂, since the values for Sno are quite different: 484.90 eV (BE) and 437.3 eV (KE), respectively. In addition, the experimental Auger parameter is closer to that expected for bulk SnO₂ (918.60 eV) than for bulk SnO (919.3 eV). Finally, the absence of an energy loss peak at -27 eV in the REELS spectra of these samples confirm that SnO is not present (Fig. 11). By contrast, in Sample 1, the main Sn3d $_{5/2}$ peak, which could be ascribed both to SnO₂ and to SnO, is accompanied by a small shoulder at 488.4 eV that must be attributed to metallic Sn (Fig. not shown).

The surfaces of the samples studied in this work highlight differentalteration degrees. Surface analyses suggest that in Sample 1, located in a non polluted rural atmosphere, the main deterioration of Hg-Sn alloy would be lower than for Samples 2, 3, 4, where the atmospheric conditions are more aggressive and, consequently, the tin oxides are formed not only at the surface but also in the bulk of these samples. This phenomenon facilitated the dealloying process of the amalgam of samples 2, 3, 4. The mercury-rich phase present in these samples, detected only by SEM/EDX analyses, accelerates the corrosion of the tin-rich solid phase. The dealloying process involves the selective leaching of mercury that slowly evaporates. Gravity also could have played a role in the formation and release of mercury drops [2]. This would explain the presence of a liquid mercury

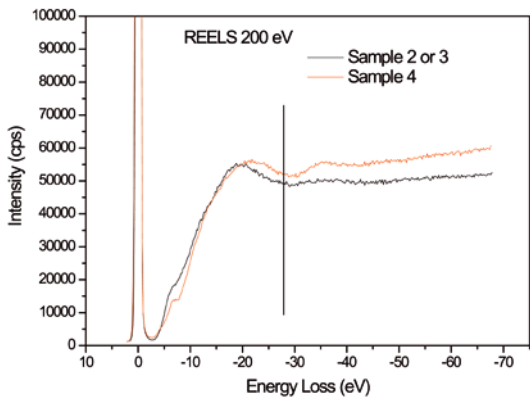


Figure 11. Electron energy loss spectra at E₀= 200 eV of Samples 2, 3 and 4

phase on the top of the craters and at the bottom edge of the mirrors. The tin-rich solid phase would be expected to oxidize after the release of mercury, which causes the softening of the amalgams [8]. The small tin particles with high specific surface area and high porosity in the samples produced by mercury release facilitated the oxidation of the bulk of the amalgam [5].

The presence of SnO_2 in the amalgams has been detected by GIXRD; in addition, Sn^{2+} and Sn^0 species have not been detected by XPS analysis on the surface. These results confirm the high degree of alteration of Samples 2 and 3. A predominant role of atmospheric pollutants such as sulphates has been detected in Sample 4, accelerating its corrosion process.

In Sample 1 any oxidized Sn phase is neither SnO nor SnO₂, suggesting better conservation or a less altered sample, which most probably is due to the surrounding environments. However, the XPS shows the presence of Sn⁴⁺ confirming the oxidation process at the sample surface, which is explained by the different penetration depth of both techniques.

4. Conclusions

The mirrors that are a part of the ornamentation of important buildings from Andalusia were made with $Hg_{0.1}Sn_{0.9}$ and β -Sn phases. According to the present study, grazing incidence X-ray diffraction (GIXRD) is a potential and useful non-destructive research tool for studying cultural heritage artefacts. The developed GIXRD experimental set—up used on the amalgam surfaces offers an unique opportunity to obtain, on the same sample and under identical conditions, a depth profile analysis that allows us to correlate information between the surface and bulk properties of the mirrors. XPS analyses reinforce the information obtained by GIXRD. In samples 2, 3 and 4 a unique chemical

species, Sn⁴⁺, was found. In sample 1, XPS analysis is the only technique that has confirmed the formation of Sn⁴⁺ at the surface. The combination of the GIXRD and XPS results demonstrate that the degradation process is driven by the surrounding environment. The sample oxidation started at the surface, causing phase degradation that varies from an oxygen rich phase at the surface to an oxygen poor one in the bulk.

Acknowledgments

This work was supported by the European Commission; Marie Curie Action MEST-CT2004-513915 and Ministry of Science and Technology of Spain, the FEDER program of the E.C. (Grants No. MAT 2007-63234, MAT 2005-04838) and (Grant MEC/FULLBRIGHT postdoct 2007). The authors are very grateful to ESRF BM25 for their assistance during our experiments (experiment EC-2502619).

References

- [1] F. Morser, Glass Ind. 42, 244 (1961)
- [2] P. Hadsund, Stud. Conserv. 38, 3 (1993)
- [3] J.M.F. Navarro, El Vidrio, 3rd edition (CSIC publications, Madrid, 2003)
- [4] H. Römich, in: N.H. Tennent (Ed.), The conservation of glass and ceramics. Research, Practice and Training (James and James Science Publishers, London, 1999)
- [5] L.K. Herrera, A. Duran, M.L. Franquelo, A. Justo, J.L. Perez-Rodriguez, J. Non-Cryst. Solids (in press)
- [6] I. De Ryck, E. Van Biezen, K. Leyssens, A. Adriaens, P. Storme, F. Adams, J. Cult. Herit. 5, 2, 189 (2004)
- [7] L. Robbiola, K. Rahmouni, C. Chiavari, C. Martini, D. Prandstraller, A. Texier, H. Takenouti, P. Vermaut, Appl. Phys. A: Mater. Sci. Process. 92, 1, 161 (2008)

- [8] L.K. Herrera, A. Duran, M.L. Franquelo, M.C. Jimenez de Haro, A. Justo, J.L. Perez-Rodriguez, J. Cult. Herit., DOI:10.1016/j. culher.2008.06.007
- [9] R.A. Ramik, R.M. Organ, J.A. Mandarino, Can. Mineral. 41, 3, 649 (2003)
- [10] S.E. Dunkle, J.R. Craig, J.D. Rimstidt, W.R. Lusardi, Geoarchaeology 19, 6, 531 (2004)
- [11] H. Strandberg, L.-G. Johansson, O. Lindqvist, Werkst korros. 48, 11, 721 (1997)
- [12] L. Robbiola, J.-M. Blengino, C. Fiaud, Corros. Sci. 40, 12, 2083 (1998)
- [13] L.K. Herrera, A. Duran, M.C. Jimenez de Haro, J.L. Perez-Rodriguez, A. Justo, Coalition Electronic Newsletter 14, 10 (2007)
- [14] J. Rubio-Zuazo, G.R. Castro, Nucl. Inst Meth A. 547, 64 (2005)
- [15] J. Rubio-Zuazo, G.R. Castro, Rev. Adv. Mater. Sci. 15, 79 (2007)
- [16] J. Rubio-Zuazo, PhD thesis, Autonomous University of Madrid (Madrid, Spain, 2005)
- [17] V.M. Jiménez, J.A. Mejías, J.P. Espinós A.R. González-Elipe, Surf. Sci. 366, 545 (1996)
- [18] H. Dosch, Critical Phenomena at Surfaces and Interfaces (Evanescent X-ray and Neutron Scattering), Springer Tracts in Modern Physics Vol. 126 (Springer, Berlin, 1992)
- [19] K.W. Evans-Lutterodt, M.T. Tang, J. Appl. Cryst. 28, 318 (1995)
- [20] R. Feidenhans'l, Surf. Sci. Rep. 10, 105 (1989)
- [21] J. Als-Nielsen, D. McMorrow, Elements of Modern X-ray Physics (Wiley, New York, 2001)
- [22] D.W. Breiby, O. Bunk, J.W. Andreasen, H.T. Lemke, M.M. Nielsen, J. Appl. Cryst. 41, 262 (2008)
- [23] M.F. Toney, S. Brennan, J. Appl. Phys. 65, 4763 (1989)
- [24] B.L. Henke, E.M. Gullikson, J.C. Davis, Atomic Data and Nuclear Data Tables 54, 2, 181 (1993)
- [25] M.C. Corbeil, Stud. Conserv. 43, 265 (1998)